Preparation of Si-C-O Ceramic Fibers from Commercial Silicon Resin

H. Li, Y. Gou*, H. Wang*, K. Jian

Science and Technology on Advanced Ceramic Fibers and Composites Laboratory, National University of Defense Technology, Changsha, Hunan, P. R. China, 410073

Abstract

Si-C-O ceramic fibers were prepared from commercial silicon resin by means of melt spinning, UV curing and pyrolysis. The composition and structure of the precursors were characterized with FT-IR and NMR. Silicon resin exhibited excellent spinning performance for use as a precursor to prepare continuous fibers. UV irradiation was employed to complete the cross-linking of the green fibers, and the mechanism of the curing process was determined with FT-IR. After pyrolysis at 1 000 °C, Si-C-O ceramic fibers were obtained, which exhibited good flexibility with 7.5 μm in diameter and 0.8 GPa in tensile strength. The obtained fibers remained amorphous below 1 300 °C. When the temperature reached above 1 300 °C, SiC with a small crystal size appeared because of carbothermal reduction, and the fiber gradually lost mechanical strength owing to the pores caused by release of low-molecular-weight molecules such as CO, CO_2 and SiO.

Keywords: Si-C-O ceramic fibers, silicon resin, precursor, low cost, UV curing

I. Introduction

Silicon-based ceramic fibers derived from polymers are used as reinforcement materials in composite applications, such as metal matrix composites and ceramic matrix composites (CMCs) [1-6]. Silicon carbide (SiC) fibers exhibit superior thermal stability and chemical resistance at high temperature, but their high cost prohibits the widespread use of SiC fibers [7-9]. Si-C-O ceramic fibers exhibit excellent stability below 1 200 °C, as well as good mechanical properties. Si-C-O is an intermediate form between SiC and SiO_2. The three elements are connected by covalent bonds and form a tetrahedral structure [10-12]. Si-C-O ceramic fibers have unique characteristics, different from both oxide fibers and non-oxide ceramic fibers. For example, with better corrosion resistance to acid or alkali than oxide fibers, Si-C-O ceramic fibers boast a much lower cost of preparation when compared with non-oxide ceramic fibers such as SiC fibers [13, 14]. Currently, commercially available Si-C-O ceramic fibers, such as Nicalon™ and Tyrano™ fibers, are exclusively prepared from expensive polycarbosilane precursors [15, 16]. The use of polycarbosilane presents several difficulties in the preparation of Si-C-O ceramic fibers. For example, the spinning and cross-linking processes need a high temperature, which makes the whole process more cumbersome. And the green fiber's fragility inhibits the use of continuous processing. Additionally, owing to low ceramic yields and the complicated preparation processes for the precursor, the resulting fibers are still expensive [17, 18].

A number of silicon resins have been investigated as a binding agent in bulk ceramic materials, a matrix source of ceramic matrix composites [19], and starting precursors for ceramic porous bodies or coatings [20]. Silicon resin is a kind of polysilsesquioxane, which has the general formula of $RSiO_{1.5}$ [21, 22]. In 1980s, Hurwitz and coworkers started the application of such silicon resins as ceramic fiber precursor [23], various polymer blends of polymethylsilsesquioxane and polyphenyl-propylsilsesquioxane were prepared with different ratios of phenylpropyl to methyl. Green fibers were hand drawn from the polymer blends and cured by UV light. After being pyrolyzed in an argon atmosphere at 1 400 °C, the Si-C-O ceramic fibers were obtained. Narisawa reported Si-C-O fibers prepared from commercial silicon resin YR3370, with vapor curing being used to accomplish cross-linking [24]. Kita reported the preparation of Si-C-O ceramic fibers from a polycarbosilane-polysiloxane blend [25-27].

In this work Si-C-O ceramic fibers were fabricated from commercial silicon resin SR8803 by means of melt spinning, curing and pyrolysis. For the cross-linking of the green fibers, ultraviolet (UV) radiation was used to accomplish the curing. The composition, structure and property of the resulted Si-C-O ceramic fibers were investigated.

II. Experimental Procedure

(1) Fiber preparation

Commercial silicon resin (SR8803, Yuanen Synthetic Material Co., Ltd, China) was used as the precursor. Green fibers were prepared on a lab-scale melt-spinning system. The silicon resin was first fed into an extruder, then heated, sheared, and pressured through a filtering system to eliminate any gels or unmelts. Then, the molten precursor

* Corresponding author: y.gou2012@hotmail.com,
whlucky2002@hotmail.com

passed through a single-capillary spinneret of 0.25 mm in diameter. The extrudate flowing precursor was then uniaxially drawn to filament, which was subsequently stretched and collected on a rotating graphite spool. The green fibers were irradiated with ultraviolet light with 254 nm in wavelength to accomplish cross-linking. Finally, the cured fibers were converted into Si-C-O ceramic fibers by pyrolysis at 1 000 °C in an inert atmosphere.

(2) Characterization

Fourier transform infrared spectra (FT-IR, KBr pellet) were recorded on a Nicolet Impact 360 FTIR spectrometer. Nuclear magnetic resonance (NMR; Bruker 510 instrument, Germany) spectra were captured using DMSO-d6 as a solvent. Gel-permeation chromatography (GPC; Waters 1515) analysis was performed using THF as eluent and polystyrene standards for calibration. Thermogravimetry mass spectrometry (TG-MS; STD Q600 V8.2 Build 100, TA Instrument Company, USA) and differential scanning calorimetry (DSC) were performed under nitrogen atmosphere (100 mL/min) at a heating rate of 10 K/min. X-ray diffraction (XRD; Bruker D8 advanced diffractometer, CuKα, Germany) measurements were conducted at ambient temperature. X-ray photoelectron spectroscopy (XPS) was performed with a Thermo ESCALAB 250 spectrometer, USA. ^{29}Si solid-state NMR spectra of the samples were obtained on a Bruker AV 300 MHz spectrometer, ^{29}Si spectra were recorded at 59.6 MHz by spinning powdered samples packed into zirconia rotors at 5 kHz with a contact time of 9 ms and a relaxation delay of 5 s, using the cross-polarization (CP) method. The diameter of the green fiber was measured with a BS-D8000 Digital Microscope (SONIC, Osaka, Japan). The morphology and microstructure of fibers were characterized using scanning electron microscopy (SEM; Hitachi S4800, Japan). The tensile strength and elastic modulus of the ceramic fibers were measured with the single filament method with a gauge length of 25 mm using an Instron-type test machine (Testometric, M350–5CT), which were obtained from the average result of 24 filaments. The chemical composition of the precursor and fibers was investigated in a series of chemical analyses. The oxygen content of the derived fibers was determined with a Horiba oxygen/nitrogen analyzer EMIA-820 (Horiba, Japan), and the carbon content with a Horiba carbon/sulfur analyzer EMIA-320 V.

III. Results and Discussion

(1) Characterization and melt spinning of the precursor

FT-IR spectrum of the precursor is shown in Fig. 1 (a). The peak at around 1 000 – 1 200 cm^{-1} belongs to Si-O-Si. The peak at 1 260 cm^{-1} can be attributed to the bending vibration of Si-C bond of Si-CH$_3$, while peaks at 1 450 cm^{-1} and 1 650 cm^{-1} belong to the bending vibration of the Si-C bond of Si-Ph. Peaks around 2 900 cm^{-1} belong to the stretching vibration of the C-H bond of -CH$_3$ and -Ph, and the peak at 3 500 cm^{-1} indicates the existence of -OH. Molecular weight and polydispersity of the silicon resin precursor were measured with GPC (Fig. 1 (b)). The broad peak indicates the heterogeneity of molecular weight distribution. The Mw is about 2 400 with a polydispersity index of 5.73.

Fig. 2 shows the NMR spectra of the precursor. In the ^{1}H NMR spectrum, the peak between 7 – 8 ppm belongs to the C-H bonds of -Ph, while the peak at 3.30 ppm belongs to -OCH$_3$. The chemical shift at 2.50 ppm can be attributed to DMSO solvent. The appearance of the peak at 2.23 ppm indicates the existence of O-H. The peaks at around -0.5 – 1.5 ppm belong to the C-H bonds of -CH$_3$. The ^{29}Si NMR spectrum of the precursor indicates a signal of SiCO$_3$ environment between -50 ppm to -80 ppm, including RSi(OSi)$_3$, RSi(OSi)$_2$(OH), RSi(OSi)$_2$(OCH$_3$), RSi(OSi)(OH)$_2$, RSi(OSi)(OCH$_3$)$_2$ and RSi(OSi)(OH)(OCH$_3$), in which R could be -CH$_3$ or -Ph. The strongest peak at -64 ppm belongs to PhSiO$_3$, while the peak at -77 ppm is assigned to CH$_3$SiO$_3$. The structure of SiCO$_3$ can be a series of permutation and combination, where "C" is from -Ph, -CH$_3$, and "O$_3$" is from –(OSi)$_3$, –(OSi)$_2$(OH), –(OSi)$_2$(OCH$_3$), –(OSi)(OH)$_2$, –(OSi)(OCH$_3$)$_2$ and –(OSi)(OH)(OCH$_3$). The structure of SiO$_4$ is confirmed by the signal at -106 ppm [28].
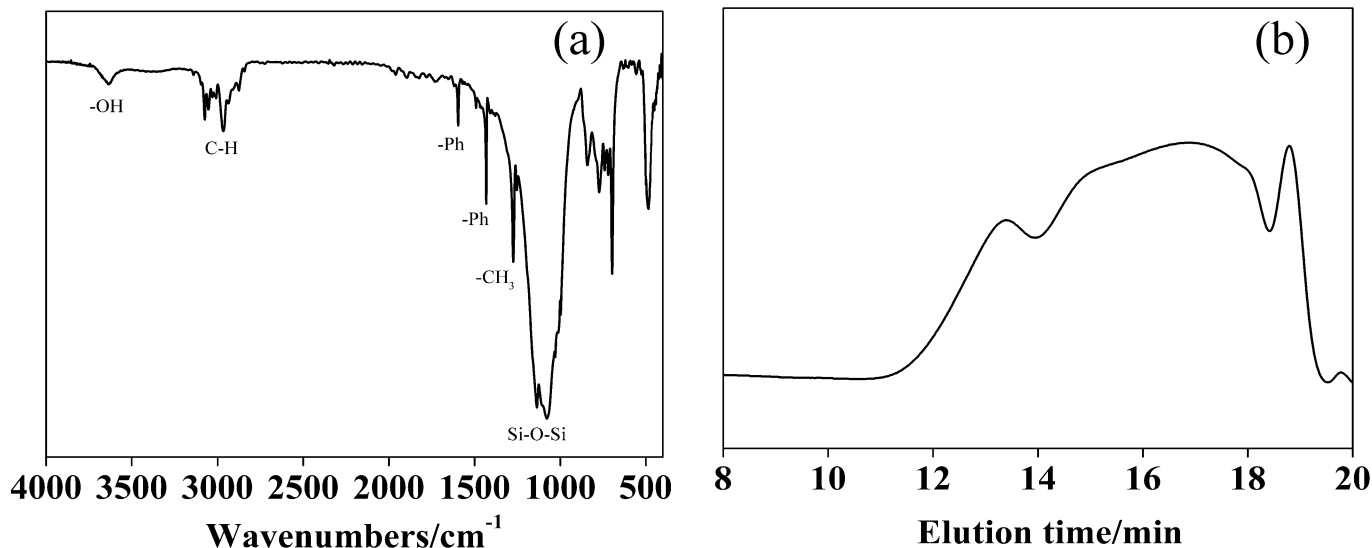

Fig. 1: (a) FT-IR spectrum and (b) GPC curve of silicon resin SR8803.
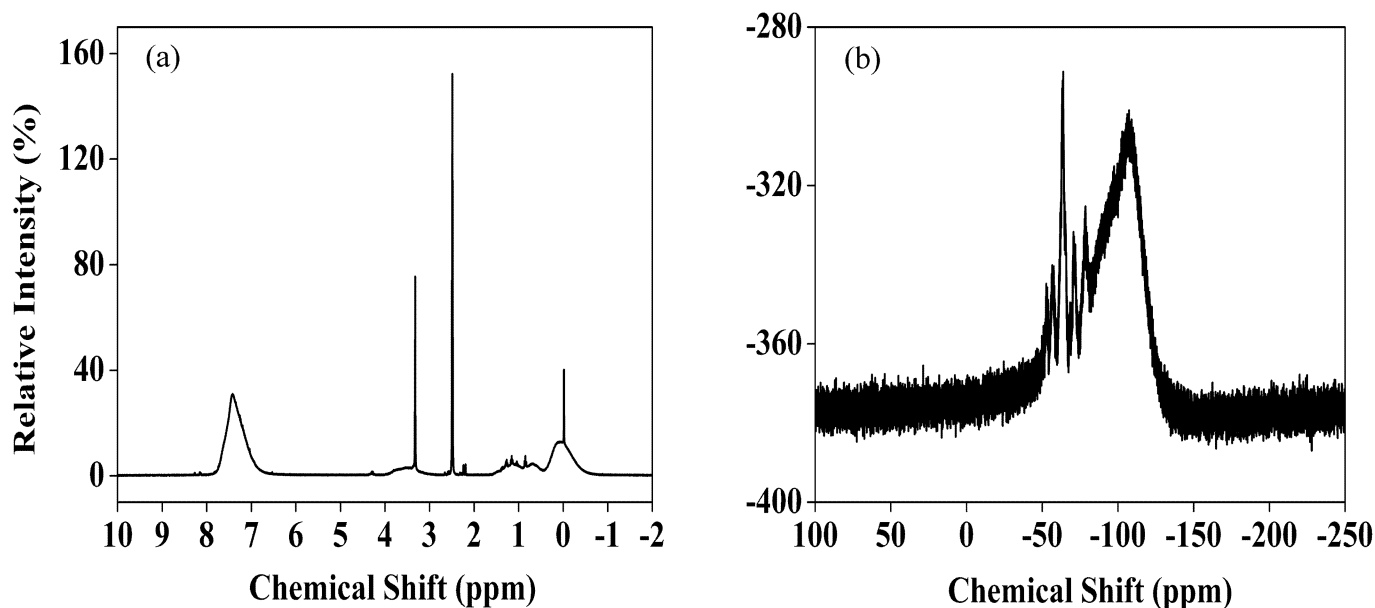
Fig. 2: (a) ^{1}H NMR and (b)^{29}Si NMR spectra of silicon resin SR8803.

According to the result of FT-IR and NMR, the silicon resin precursor is confirmed to have the backbone of Si-O-Si, with side chains of -CH$_3$, -OCH$_3$, -Ph and -OH (Fig. 3).
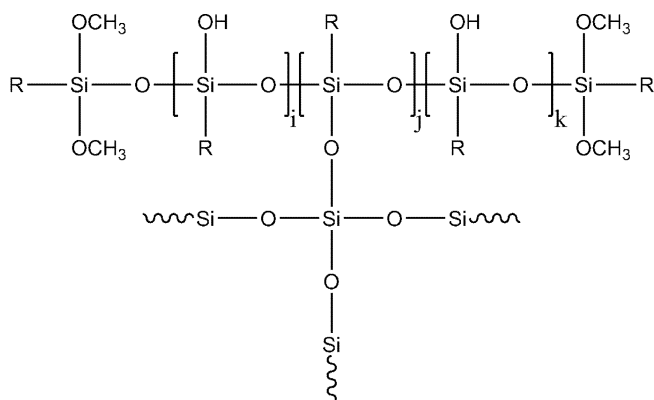

Fig. 3: Structure of silicon resin SR8803.

The TG-MS of the precursor is shown in Fig. 4. The precursor has a high ceramic yield of 73.2 wt% at 1 000 °C in an inert atmosphere, which indicates the suitability of silicon resin for use as a precursor to prepare ceramic fibers. From the results of MS, the evaporation of H$_2$O between 100 ~ 300 °C can be detected. The loss of CH$_4$ appears when the temperature rises to 700 – 900 °C. The release of CH$_4$ and C$_6$H$_6$ can be attributed to the decomposition of the side chains, and the escape of CO$_2$ could be explained with the ceramization process [29, 30].

Owing to the low potential barrier of axis rotation and linearization of Si-O-Si in backbone, silicon resin exhibits a better spinning property compared with other polymers. Continuous melt spinning of silicon resin was successfully performed at 150 °C. Fig. 5 shows the optical photograph of the obtained green fibers. The average diameter of the green fibers is 14 μm.
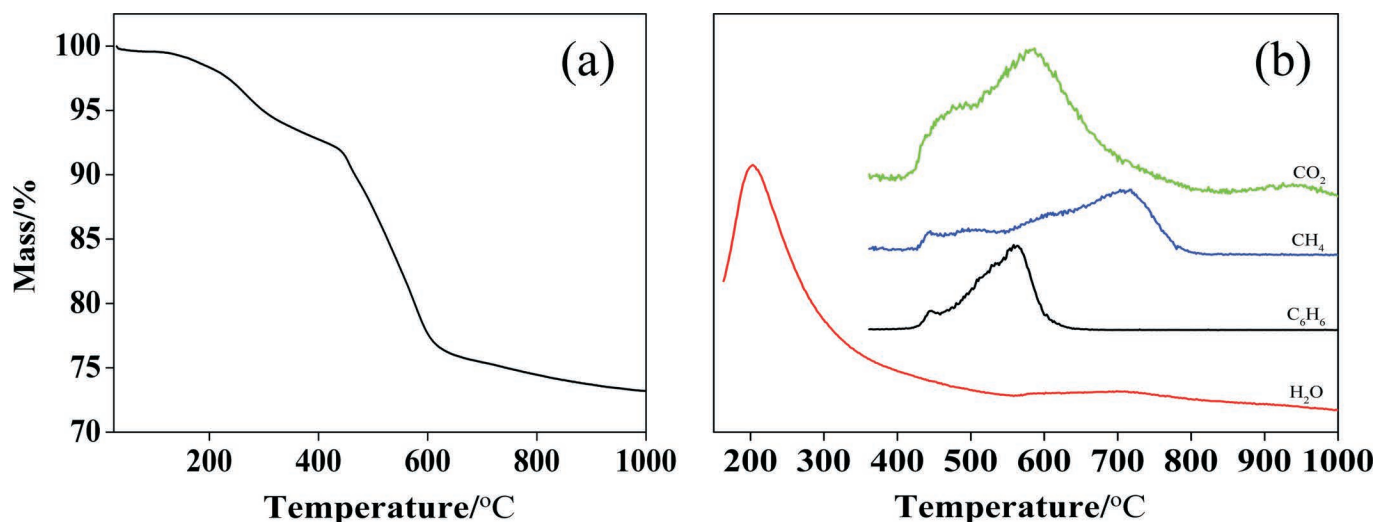

Fig. 4: TG graph (a) and MS graph (b) of the silicon resin SR8803.

Fig. 5: Optical photograph of the green fibers.

(2)   Curing and pyrolysis process

Thermal oxidation curing was performed on the green fibers with the temperature up to 200 °C. During the heating process, however, the fibers were completely melted down. It could be easily explained by the intrinsic softening temperature of silicon resin (75.8 °C). In order to complete the curing process below softening temperature, fibers were irradiated with ultraviolet light of 254 nm in wavelength. The FT-IR spectrum in Fig. 6 shows the disappearance of C-H at around 2 900 cm^{-1} after the curing process, and a new peak appears at 1 730 cm^{-1}, which can be attributed to C=O bond owing to the oxidation of side chains.

The cured fibers were pyrolyzed at 1 000 °C in an inert atmosphere, and maintained at 1 000 °C for 1 h to obtain Si-C-O ceramic fibers. The FT-IR spectrum of the ceramic fibers shows that all the peaks of organic groups have disappeared (Fig. 6), indicating that the ceramization process has been completed.

Fig. 7 shows the TG and MS graphs of the cured fibers. The cured fiber has a ceramic yield of 86.2 wt% at 1 000 °C in an inert atmosphere, which is much higher than that of the precursor (73.2 wt%). In the results of MS, the evaporation of CH_4 and C_6H_6 disappear as there is no C-H after cross-linking. The escape of CO_2 can be detected between 500 – 650 °C, which can be attributed to the decomposition of C = O [31, 32].
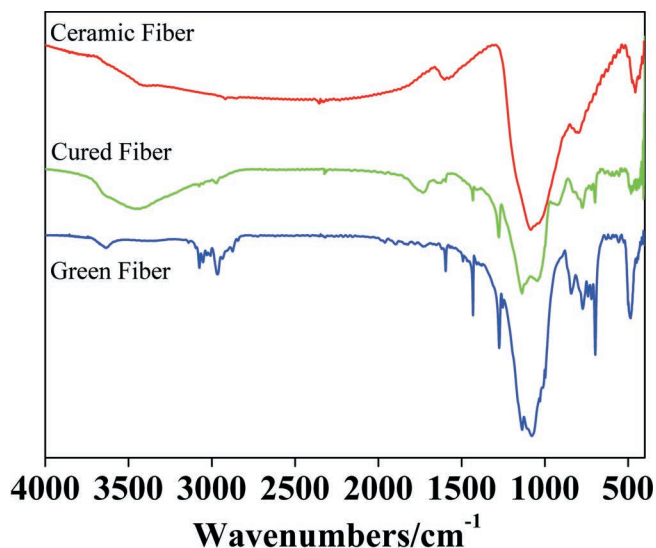

Fig. 6: FT-IR spectrum of green fiber, cured fiber and ceramic fiber.

(3)   Properties of Si-C-O ceramic fibers

Table 1 details the composition of the silicon resin precursor and the as-obtained ceramic fibers pyrolyzed at 1 000 °C. Although the precursor has a high content of carbon, after pyrolysis, the carbon content decreases in the Si-C-O ceramic fibers, and the percentage of Si and O increases slightly.
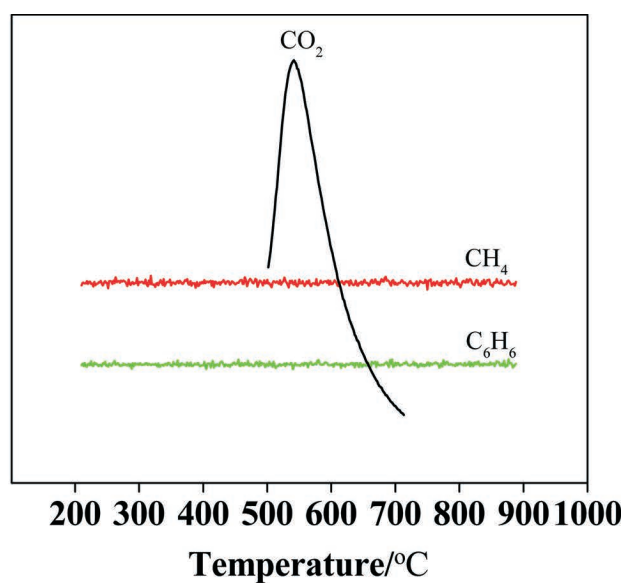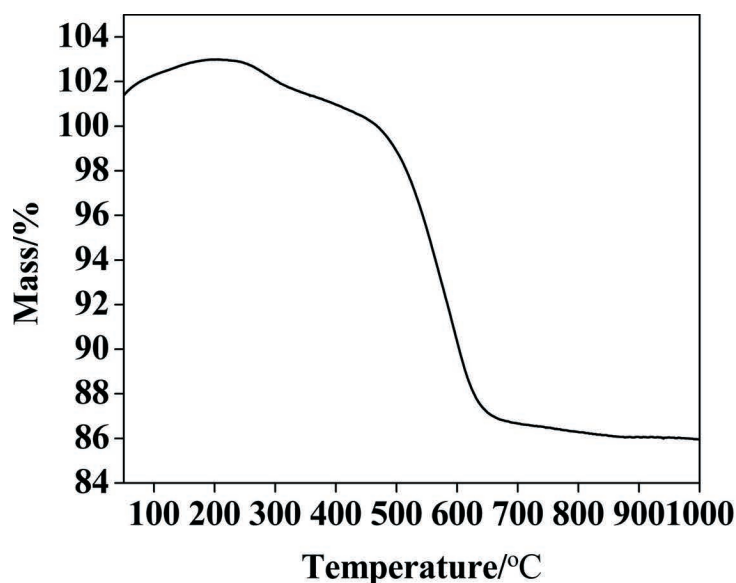

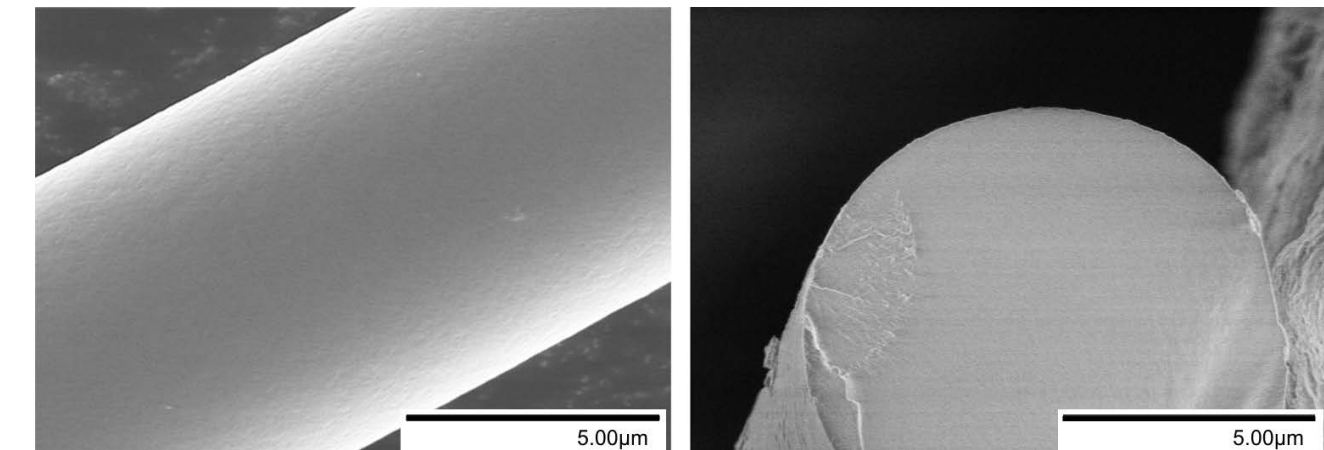**Fig. 7:** TG graph (a) and MS graph (b) of the cured fiber.

Fig. 8: SEM graph of the as-obtained Si-C-O ceramic fiber.

Table 1: Elemental composition of the precursor and as-obtained Si-C-O ceramic fibers.

Samples	Composition [wt%]			Formula
	Si	C	O	
SR8803 precursor	26.89	46.43	17.85	$SiC_{4.2}O_{1.2}$
Si-C-O ceramic fiber	39.09	33.54	25.86	$SiC_{2.1}O_{1.2}$

Fig. 8 shows the morphologies of the surface and cross-section of the as-obtained Si-C-O ceramic fibers. As can be seen from the micrographs, the fiber has smooth surfaces and a densified structure. After pyrolysis at 1 000 °C, the diameter was reduced to 7.5 μm from 14 μm. The as-obtained Si-C-O ceramic fibers have an average tensile strength of 0.8 GPa and elastic modulus of 100 GPa.

The XPS spectrum of the Si-C-O ceramic fiber is shown in Fig. 9. Peaks at 103.1eV, 154.1eV, 284.3eV, 532.4eV belong to Si2p, Si2s, C1s and O1s, respectively. Simulation of the XPS graph reveals that the element C in the Si-C-O ceramic fiber exists as C-C and SiC_xO_y. The high content of C-C bond reveals that the element C mainly exists in the form of free carbon. The element Si in the Si-C-O ceramic fiber exists mainly as SiO_2 and SiC_xO_y [33, 34].
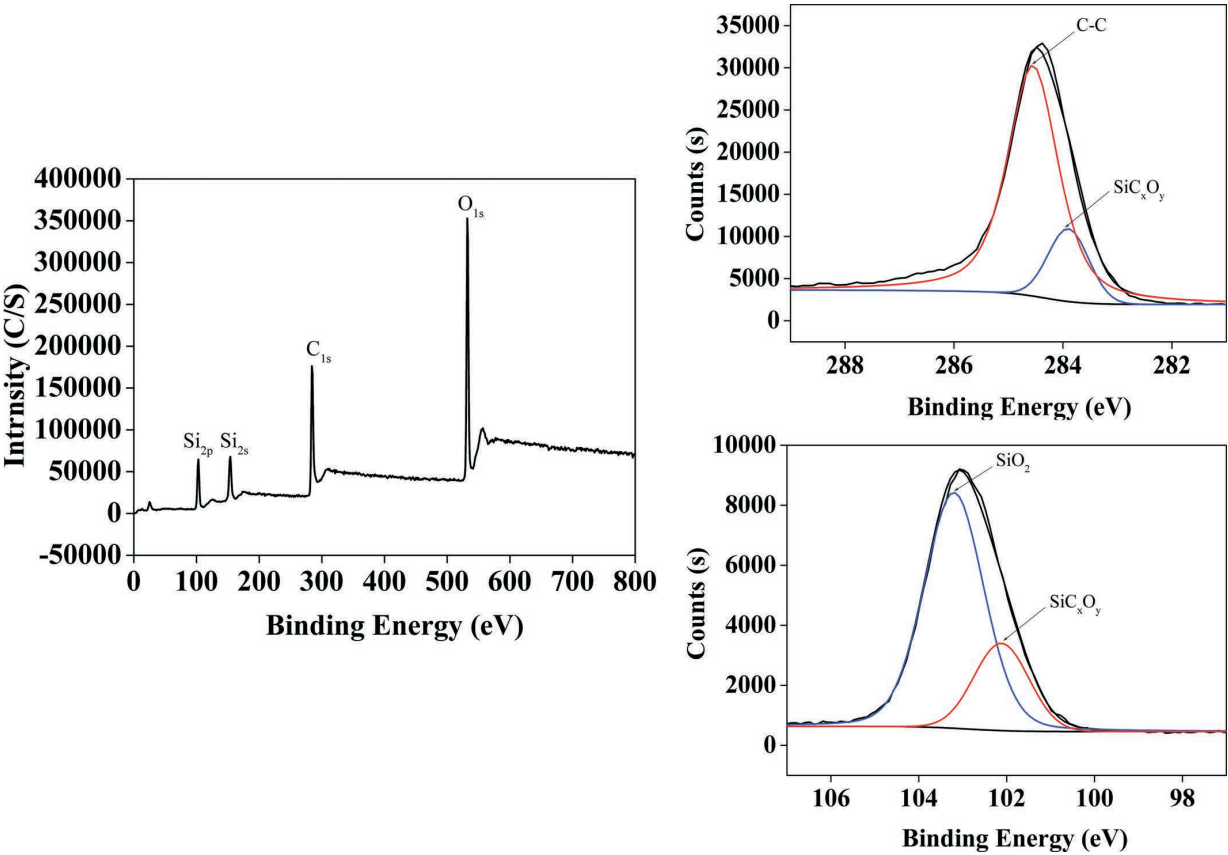

Fig. 9: XPS spectrum of the Si-C-O ceramic fiber and C1s, Si2p simulated curves.

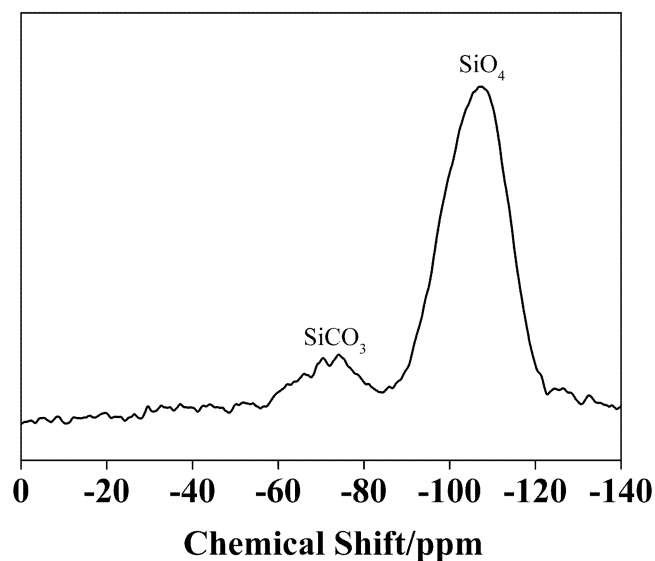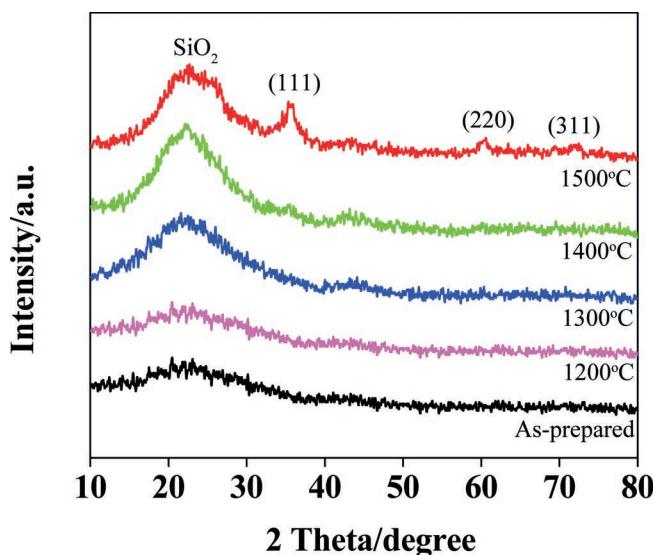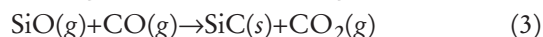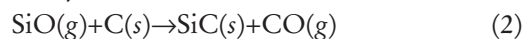**Fig. 10:** ^{29}Si solid-state NMR spectrum of the Si-C-O ceramic fiber.

Fig. 11: XRD patterns for the as-prepared Si-C-O ceramic fiber and samples annealed at 1 200 °C, 1 300 °C, 1 400 °C, and 1 500 °C.

The ^{29}Si solid-state NMR spectrum is used to further confirm the structure of the Si-C-O ceramic fiber (Fig. 10). The result shows the structure of SiO_4 derived from SiO_2 and the structure of $SiCO_3$ derived from SiC_xO_y phase, which is consistent with the result of XPS.

The as-obtained Si-C-O ceramic fibers were annealed at different temperatures for 2 h to investigate the thermal properties and crystallization behavior.

XRD patterns for the as-prepared Si-C-O ceramic fiber and samples annealed at different temperatures are shown in Fig. 11. The as-prepared sample is amorphous and remains amorphous up to 1 300 °C, which indicates the good stability of Si-C-O ceramic fibers below 1 300 °C. As the temperature reaches 1 400 °C, SiC with a small crystallite size appears owing to the carbothermal reduction [35–37], and the fibers lose mechanical strength owing to the pores caused by evolution of low-molecular-weight molecules such as CO, CO_2 and SiO.

To further prove the occurrence of carbothermal reduction, a DSC test was conducted. The result is shown in Fig. 12. It could be seen that there is an obvious exothermic peak at 1 350 °C, which can be attributed to the following carbothermal reduction as reported in the literature [38].

$$SiC_xO_y(s) \rightarrow SiO(g) + CO(g) + C(s) \qquad (1)$$

$$SiO(g) + C(s) \rightarrow SiC(s) + CO(g) \qquad (2)$$

$$SiO(g) + CO(g) \rightarrow SiC(s) + CO_2(g) \qquad (3)$$

The micrographs of Si-C-O ceramic fibers annealed at different temperatures are shown in Fig. 13. The surface of the fibers shows a dense structure and crystallization is not observed at 1 300 °C. After exposure at 1 400 °C, the surface is wrinkled and a porous texture appears caused by the release of gases [39].
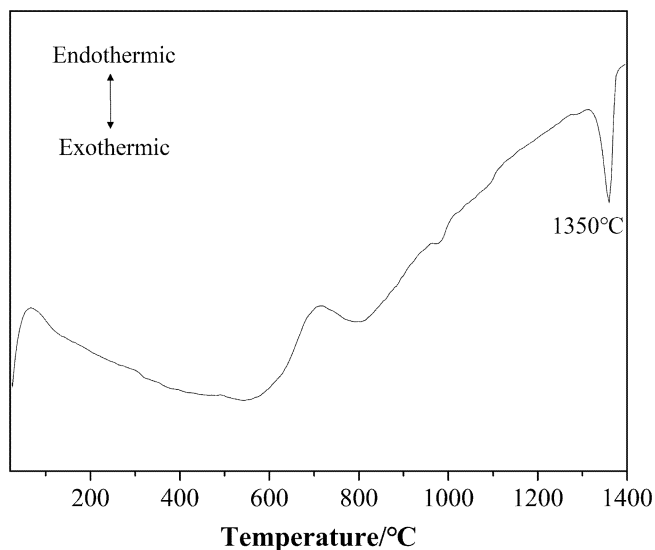

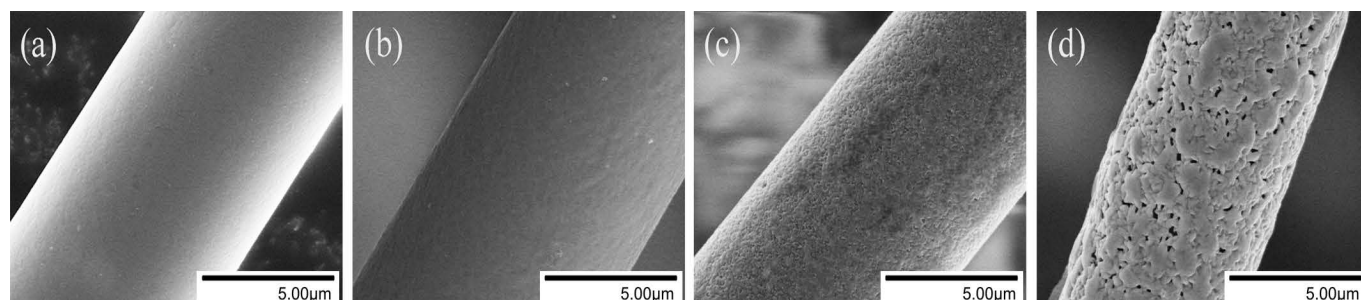**Fig. 12:** DSC graph of fibers after curing.

Fig. 13: SEM graph of the Si-C-O ceramic fiber annealed at 1 200 °C (a), 1 300 °C (b), 1 400 °C (c), and 1 500 °C (d).

IV. Conclusions

A polymer-derived method is employed to prepare Si-C-O ceramic fibers using commercial silicon resin SR8803. The silicon resin has a backbone of Si-O-Si, with side chains of -CH$_3$, -OCH$_3$, -Ph and -OH. Green fibers with a diameter of 14 μm are obtained by means of melt spinning at 150 °C. UV irradiation is used to render the green fibers infusible. FT-IR spectrum confirms that UV irradiation completes the curing process by oxidizing side groups of the silicon resin. After the pyrolysis process of the cured fibers at 1 000 °C, Si-C-O ceramic fibers are obtained, with an average tensile strength of 0.8 GPa and elastic modulus of 100 GPa. SEM images show the fibers have a smooth surface and densified structure. XPS and ^{29}Si solid-state NMR spectrum indicate the structure of SiO$_2$ and SiC$_x$O$_y$. The Si-C-O ceramic fibers remain amorphous below 1 300 °C, XRD patterns indicate that SiC with a small crystallite size starts to appear at 1 400 °C, and the surface starts to become wrinkled. Fibers lose mechanical properties gradually as the temperature rises owing to the pores caused by evolution of low molecular weight molecules such as CO, CO$_2$ and SiO during the carbothermal reduction.

References

[1] Yajima, S., Hasegawa, Y., Okamura, K., Matsuzawa, T.: Development of high tensile strength silicon carbide fiber using an organosilicon polymer precursor, *Nature*, **273**, 525–527, (1978).

[2] Quemard, L., Rebillat, F., Guette, A., Tawil, H., Louchet-Pouillerie, C.: Self-healing mechanisms of a SiC fiber reinforced multi-layered ceramic matrix composite in high pressure steam environments, *J. Eur. Ceram. Soc.*, **27**, 2085–2094, (2007).

[3] Ji, X., Wang, S., Shao, C., Wang, H.: High-temperature corrosion behavior of SiBCN fibers for aerospace applications, *ACS Appl. Mater. Inter.*, **10**, 19712–19720, (2018).

[4] Lipowitz, J.: Structure and properties of ceramic fibers prepared from organosilicon polymers, *J. Inorg. Organomet. P.*, **1**, 277–297, (1991).

[5] Colombo, P., Mera, G., Riedel, R., Soraru, G.D.: Polymer-derived ceramics: 40 years of research and innovation in advanced ceramics, *J. Am. Ceram. Soc.*, **93**, 1805–1837, (2010).

[6] Ji, X., Shao, C., Wang, H. *et al.*: A simple and efficient method for the synthesis of SiBNC ceramics with different Si/B atomic ratios, *Ceram. Int.*, **43**, 7469–7476, (2017).

[7] Gou, Y., Wang, H., Jian, K.: Formation of carbon-rich layer on the surface of SiC fiber by sintering under vacuum for superior mechanical and thermal properties, *J. Eur. Ceram. Soc.*, **37**, 907–914, (2016).

[8] Xie, Z., Gou, Y.: Polyaluminocarbosilane as precursor for aluminium-containing SiC fiber from oxygen-free sources, *Ceram. Int.*, **42**, 10439–10443, (2016).

[9] Gou, Y., Wang, H., Jian, K., Song, Y., Wang, J.: The investigation of properties of SiC ceramic fibers with various composition and structure, *Mater. Sci. Forum*, **816**, 163–165, (2015).

[10] Mera, G., Riedel, R., Sen, S. *et al.*: Polymer-derived SiCN and SiOC ceramics-structure and energetics at the nanoscale, *J. Mater. Chem. A.*, **1**, 3826–3836, (2013).

[11] Kroll, P.: Searching insight into the atomistic structure of SiCO ceramics, *J. Mater. Chem.*, **20**, 10528–10534, (2010).

[12] Zhang, H., Pantano, C.G.: Synthesis and characterization of silicon oxycarbide glasses, *J. Am. Ceram. Soc.*, **73**, 958–963, (1990).

[13] Soraru, G.D., Dallapiccola, E., Andrea, G.D.: Mechanical characterization of sol-gel-derived silicon oxycarbide glasses, *J. Am. Ceram. Soc.*, **79**, 2074–2080, (1996).

[14] Kleebe, H.J., Truquat, C., Soraru, G.D.: Phase separation in an SiCO glass studied by transmission electron microscopy and electron energy-loss spectroscopy, *J. Am. Ceram. Soc.*, **84**, 1073–1080, (2001).

[15] Bodet, R., Jia, N., Tressler, R.E.: Microstructural instability and the resultant strength of SiCO (Nicalon) and SiNCO (HPZ) fibres, *J. Eur. Ceram. Soc.*, **16**, 653–664, (1996).

[16] Bunsell, A., Piant, A.: A review of the development of three generations of small diameter silicon carbide fibers, *J. Mater. Sci.*, **41**, 823–839, (2006).

[17] Bujalski, D.R., Su, K., Zank, G.A.: Process of producing fibers from curable alk-1-enyl ether functional siloxane resins, U.S. Pat. No. 5,814,271.

[18] Atwell, W.H., Bujalski, D.R., Joffre, E.J. *et al.*: Preparation of substantially polycrystalline silicon carbide fibers from poly-organosiloxanes, U.S. Pat. No. 5,167,881.

[19] Rahimi, A., Shokrolahi, P.: Application of inorganic polymeric materials: polysiloxanes, *J. Inorg. Mater.*, **3**, 843–847, (2001).

[20] Brus, J., Kolar, F., Machovic, V. *et al.*: Structure of silicon oxycarbide glasses derived from poly(methylsiloxane) and poly[methyl(phenyl)siloxane]precursors, *J. Non-Cryst. Solids*, **289**, 62–74, (2001).

[21] Bujalski, D.R., Chen, H., Ronald, E. *et al.*: Compositional and structural analysis of a (PhSiO$_{3/2}$)$_{0.35}$(MeSiO$_{3/2}$)$_{0.40}$ (Me$_2$ViSiO$_{1/2}$)$_{0.25}$ resin, *Macromolecules*, **36**, 180–197, (2003).

[22] Bujalski, D.R., Chen, H., Zank, A. *et al.*: Synthesis of (PhSiO$_{3/2}$)$_{0.35}$(MeSiO$_{3/2}$)$_{0.40}$(Me$_2$ViSiO$_{1/2}$)$_{0.25}$ resins, *Macromolecules*, **36**, 3529–2539, (2003).

[23] Hurwitz, F.I., Farmer, S.C., Terepka, F.M. *et al.*: Silsesquioxanes-derived ceramic fibers, *J. Mater. Sci.*, **26**, 1247–1252, (1991).

[24] Narisawa, M., Satoh, Y., Sumimoto, R. *et al.*: Synthesis of SiOC base fibers from silicone resin with low carbon content and control of surface functionality by metal chloride treatment in vapor, *Mater. Sci. Forum*, **658**, 400–403, (2010).

[25] Kita, K., Narisawa, M., Mabuchi, H.: Melt spinnable blend polymers of polycarbosilane and polysiloxane for synthesis of silicon carbide micro tube structures, *Key. Eng. Mater.*, **352**, 69–72, (2007).

[26] Kita, K., Narisawa, M., Mabuchi, H.: Formation of continuous pore structures in Si-C-O fibers by adjusting the melt spinning condition of a polycarbosilane-polysiloxane polymer blend, *J. Am. Ceram. Soc.*, **92**, 1192–1197, (2009).

[27] Narisawa, M., Sumimoto, R., Kita, K. *et al.*: Investigation of curing process on melt spun polymethylsilsesquioxane fiber as precursor for silicon oxycarbide fibers, *Adv. Mater. Res.*, **66**, 1–4, (2009).

[28] Narisawa, M., Sumimoto, R., Kita, K. *et al.*: Melt spinning and metal chloride vapor curing process on polymethyl-

silsesquioxane as Si-C-O fiber precursor, *J. Appl. Polym. Sci.*, **114**, 2600 – 2607, (2009).

29   Riedel, R.: Nanoscaled inorganic materials by molecular design, *Chem. Soc. Rev.*, **41**, 5029 – 5031, (2012).

30   Statheropoulos, M., Kyriakou, S., Tzamtzis, N.: Performance evaluation of a TG/MS system, *Thermochim. Acta.*, **322**, 167 – 173, (1998).

31   Ji, X., Shao, C., Wang, H., Cheng, J., Li, H.: Curing green fibres infusible by electron beam irradiation for the preparation of SiBNC ceramic fibres, *Ceram. Int.*, **43**, 11218 – 11224, (2017).

32   Li, H., Gou, Y., Chen, S., Wang, H.: Synthesis and characterization of soluble and meltable Zr-containing polymers as the single-source precursor for Zr(C, N) multinary ceramics, *J. Mater. Sci.*, **53**, 10933 – 10945, (2018).

33   Cheng, J., Wang, X., Wang, H., Shao, C., Wang, J.: Preparation and high temperature behavior of HfC-SiC nanocomposites derived from a non-oxygen single-source-precursor, *J. Am. Ceram. Soc.*, **100**, 5044 – 5055, (2017).

34   Li, H., Gou, Y., Chen, S., Wang, H.: Preparation and properties of a novel precursor-derived Zr-C-B-N composite ceramic via zirconocene and borazine, *Ceram. Int.*, **44**, 4097 – 4104, (2018).

35   Narisawa, M., Sumimoto, R., Kita, K. *et al.*: Evaluation of oxidation resistance of thin continuous silicon oxycarbide fiber derived from silicone resin with low carbon content, *J. Mater. Sci.*, **45**, 5642 – 5648, (2010).

36   Burns, G.T., Taylor, R.B., Xu, Y. *et al.*: High-temperature chemistry of the conversion of siloxanes to silicon carbide, *Chem. Mater.*, **4**, 1313 – 1323, (1992).

37   Vix-Guterl, C., Alix, I., Ehrburger, P.: Synthesis of tubular silicon carbide (SiC) from a carbon-silica material by using a reactive replica technique: mechanism of formation of SiC, *Acta. Mater.*, **52**, 1639 – 1651, (2004).

38   Cheng, J., Wang, J., Wang, X., Wang, H.: Preparation and high-temperature performance of HfC-based nanocomposites derived from precursor with Hf-(O,N) bonds, *Ceram. Int.*, **43**, 7159 – 7165, (2017).

39   Gou, Y., Wang, H. Jian, K. *et al.*: Preparation and characterization of SiC fibers with diverse electrical resistivity through pyrolysis under reactive atmospheres, *J. Eur. Ceram. Soc.*, **37**, 517 – 522, (2017).